ACTA ONCOLOGICA
2019, VOL. 58, NO. 10, 1463–1469
https://doi.org/10.1080/0284186X.2019.1627416

Taylor & Francis
Taylor & Francis Group

ORIGINAL ARTICLE

Towards FLASH proton therapy: the impact of treatment planning and machine characteristics on achievable dose rates

Steven van de Water[a], Sairos Safai[a], Jacobus M. Schippers[a,b], Damien C. Weber[a,c,d] and Antony J. Lomax[a,e]

[a]Center for Proton Therapy, Paul Scherrer Institute, Villigen, Switzerland; [b]Department of Radiation Therapy, Rijksuniversiteit Groningen, Groningen, the Netherlands; [c]Department of Radiation Oncology, University Hospital of Bern, Bern, Switzerland; [d]Department of Radiation Oncology, University Hospital of Zürich, Zürich, Switzerland; [e]Department of Physics, ETH Zürich, Zürich, Switzerland

ABSTRACT

Background: This study aimed at evaluating spatially varying instantaneous dose rates for different intensity-modulated proton therapy (IMPT) planning strategies and delivery scenarios, and comparing these with FLASH dose rates (>40 Gy/s).

Material and methods: In order to quantify dose rates in three-dimensions, we proposed the 'dose-averaged dose rate' (DADR) metric, defined for each voxel as the dose-weighted mean of the instantaneous dose rates of all spots (i.e., pencil beams). This concept was applied to four head-and-neck cases, each planned with clinical (4 fields) and various spot-reduced IMPT techniques: 'standard' (4 fields), 'arc' (120 fields) and 'arc-shoot-through' (120 fields; 229 MeV only). For all plans, different delivery scenarios were simulated: constant beam intensity, variable beam intensity for a clinical Varian ProBeam system, varied per energy layer or per spot, and theoretical spot-wise variable beam intensity (i.e., no monitor/safety limitations). DADR distributions were calculated assuming 2-Gy or 6-Gy fractions.

Results: Spot-reduced plans contained 17–52 times fewer spots than clinical plans, with no deterioration of plan quality. For the clinical plans, the mean DADR in normal tissue for 2-Gy fractionation was 1.7 Gy/s (median over all patients) at maximum, whereas in standard spot-reduced plans it was 0.7, 4.4, 7.1, and 12.1 Gy/s, for the constant, energy-layer-wise, spot-wise, and theoretical spot-wise delivery scenarios, respectively. Similar values were observed for arc plans. Arc-shoot-through planning resulted in DADR values of 3.0, 6.0, 14.1, and 24.4 Gy/s, for the abovementioned scenarios. Hypofractionation (3×) generally resulted in higher dose rates, up to 73.2 Gy/s for arc-shoot-through plans. The DADR was inhomogeneously distributed with highest values at beam entrance and at the Bragg peak.

Conclusion: FLASH dose rates were not achieved for conventional planning and clinical spot-scanning machines. As such, increased spot-wise beam intensities, spot-reduced planning, hypofractionation and arc-shoot-through plans were required to achieve FLASH compatible dose rates.

ARTICLE HISTORY
Received 1 April 2019
Accepted 22 May 2019

Introduction

Radiotherapy treatments delivered at dose rates exceeding 40 Gy/s, so-called 'FLASH' radiotherapy, could potentially result in improved healthy tissue sparing, while maintaining effectiveness in eradicating tumor cells. This widening of the therapeutic window has been demonstrated in pre-clinical animal experiments using electron beams [1–3], and for photons produced by a synchrotron [4]. For proton radiotherapy, a recent study, exposing normal cells *in vitro* to ultra-high dose rates, showed that FLASH irradiation provided an improvement in late adverse biological effects, even though little effect was observed on acute cell damage [5]. Whether these encouraging results can be translated into improved clinical outcomes in actual patient treatments should still be addressed in future research however, as should uncovering the radiobiological mechanism behind FLASH radiotherapy [6,7].

Since the basic infrastructure (i.e., accelerator, beamline, and gantry) of most modern proton pencil-beam scanning (PBS) facilities should in theory be able to produce proton beams at very high beam intensities [8], this also raises the question whether FLASH dose rates can be achieved for clinical proton therapy treatments. This will depend on the specifications of the PBS machine, as achievable beam intensities can be limited due to monitor system characteristics and/or safety requirements. For example, some (commercial) machines require a minimum duration for each proton spot (i.e., individual pencil beam) and therefore operate with variable beam intensities, with the intensity being varied per spot or per energy layer [9]. Consequently, achievable dose rates will also depend on the treatment plan delivered. In general, treatment plans containing high-energy spots (as beamline transport is typically more efficient at higher energies [10]) and high-weighted spots (for PBS machines with

CONTACT Steven van de Water steven.vandewater@psi.ch Center for Proton Therapy, Paul Scherrer Institute, Forschungsstrasse 111, 5232 Villigen PSI, Switzerland

Supplemental data for this article can be accessed here.

variable beam intensity) are more likely to result in proton dose rates compatible with FLASH irradiation.

The aim of this study is to assess whether FLASH dose rates (>40 Gy/s) can be obtained for clinical proton PBS treatments, and to investigate the impact of different treatment planning strategies and delivery scenarios on achievable dose rates. For this purpose, and to account for the sequential delivery of discrete proton spots, we introduced a 'dose-averaged dose rate' (DADR) metric for calculating and visualizing 3D instantaneous dose rate distributions in patient geometries. This has been applied to four patient cases, for each of which we considered the clinical plan and three additional treatment plans that were anticipated to have favorable dose rate characteristics. All treatment plans were evaluated for realistic and hypothetical delivery scenarios for two clinical PBS machines at our institute.

Material and methods

Patient data

Data from four head-and-neck cancer patients previously treated in the sinonasal region at the Paul Scherrer Institute (PSI) were included. In all cases, the clinical target volume (CTV, median: 142 cm^3, range: 114–261 cm^3) was isotropically expanded by 5 mm to create the planning target volume (PTV, median: 246 cm^3, range: 202–453 cm^3). The eyes, lenses, optic nerves, chiasm, cochlea, brainstem, spinal cord, lacrimal glands and parotid glands were, when delineated, included during optimization as organs-at-risk (OARs).

Treatment plans

For all patient cases, four intensity-modulated proton therapy (IMPT) treatment plans were considered:

1. The clinical treatment plan
2. A 'standard' spot-reduced plan
3. An 'arc' spot-reduced plan
4. An 'arc-shoot-through' spot-reduced plan

Clinical treatment plans

The clinical IMPT treatment plans were generated for delivery on PSI Gantry 2 using the in-house developed treatment planning system (TPS) 'PSIplan' [11,12]. All clinical plans contained four fields, typically arranged according to a 'star arrangement' with gantry angles of around 70°, 110°, 250°, and 290°, and 20° couch kick in superior direction. A 42 mm (water-equivalent) pre-absorber was used for all fields. More details on clinical treatment plan generation are provided in the Supplementary Material.

Spot-reduced treatment plans

The three spot-reduced treatment plans for each patient were generated using a research TPS, based on the open-source toolkit 'matRad' [13] with in-house developed extensions for IMPT optimization. The system uses the so-called 'pencil beam resampling' paradigm [14]. This means that the IMPT optimization is performed repeatedly in an iterative process, optimizing a randomly selected subset of candidate spots in each iteration, instead of the traditional approach in which candidate spots are optimized all together in a single optimization run. A detailed description of spot-reduced treatment planning can be found in the Supplementary Material.

The standard spot-reduced plans were generated using the corresponding clinical 4-field setup. For the arc plans, we approximated a continuously rotating gantry by using a coplanar 120-field arrangement with a 3-degree gantry angle separation and 0-degree couch angle, whereas for the arc-shoot-through plans, only spots with the maximum energy of 229 MeV were sampled and the pre-absorber was omitted. In all spot-reduced treatment plans, PTV coverage and dose homogeneity of $V_{95\%} > 95\%$ and $V_{107\%} < 2\%$ were required, while we tried to mimic the corresponding clinical plans by setting the clinically achieved PTV field dose homogeneity and OAR dose parameters as planning objectives. The clinical beam model of PSI Gantry 2 was also used during spot-reduced treatment planning.

Dose-averaged dose rate distributions

After normalizing the treatment plans with respect to the mean PTV dose, 3D dose-averaged dose rate (DADR) distributions were calculated according to Equation 1.

$$DADR_i = \sum_{j=1}^{n} \frac{(d_{ij}w_j)(d_{ij}BI_j)}{\sum_{j=1}^{n} d_{ij}w_j}, \quad (1)$$

where:

DADR dose-averaged dose rate [Gy/s];
i voxel;
j spot;
w spot weight [protons];
d dose-influence matrix [Gy/proton];
BI beam intensity [protons/s].

That is, for each voxel, the instantaneous dose rate is averaged over all spots, while being weighted by the dose contribution of each spot to the voxel.

Delivery scenarios

DADR distributions for all patients and treatment plans have been calculated assuming the following delivery scenarios and/or PBS machines:

1. Constant beam intensity – PSI Gantry 2 (clinical mode)
2. Variable beam intensity – PSI Gantry 3:
   a. 'Energy-layer-wise' intensity (clinical mode)
   b. 'Spot-wise' intensity (hypothetical scenario)
   c. 'Theoretical' spot-wise intensity (hypothetical scenario, no monitor/safety limitations)

The delivery scenarios above were considered for fractions of 2 Gy (conventional) and 6 Gy (hypofractionation), taking into account a constant radiobiological effectiveness of 1.1.

Constant beam intensity

The beam intensity of PSI Gantry 2 (developed in-house) ranges from $1.4*10^9$ to $2.9*10^9$ protons/s for energies of 73–229 MeV, as depicted in Figure S2 (Supplementary Material). The beam intensity is constant in the sense that, for a certain proton energy, it always has the same value irrespective of spot weight (i.e., number of protons that are delivered). The intensity values are relatively low and can be considered a conservative approach with regard to patient safety and delivery precision. The minimum deliverable spot weight of Gantry 2 is $0.2*10^6$–$0.4*10^6$ protons (for 73–229 MeV).

Variable beam intensity

On PSI Gantry 3 (Varian ProBeam, Varian Medical Systems, Palo Alto, CA, USA), the beam intensity is varied such that the delivery of each spot takes at least 3 ms. As a result, the achievable beam intensity increases with spot weight, up to the maximum intensity ranging between $8.2*10^9$, $30.2*10^9$, and $16.3*10^9$ protons/s for energies of 73, 169, and 229 MeV, respectively (see Figure S2, Supplementary Material). To limit the variation in beam intensity with energy and to ensure patient safety, maximum clinical intensities are intentionally restricted for proton energies above 169 MeV, whereas increased cyclotron output (>800 nA) can be requested for energies below 110 MeV if the accelerator permits.

In a clinical delivery mode, beam intensities are varied per energy layer ('energy-layer-wise'), with the intensity depending on the lowest weighted spot in each energy layer. The hypothetical scenario in which beam intensities can be varied per spot ('spot-wise') was also evaluated [15], as this is likely to provide higher dose rates. The minimum spot weight of Gantry 3 is higher compared with Gantry 2, varying between $2.1*10^6$ and $4.6*10^6$ protons (for 73–229 MeV). The clinical plans, originally generated for Gantry 2, contained many spots below the minimum spot weight of Gantry 3 (25–85%) and were consequently not evaluated for these 'energy-layer-wise' and 'spot-wise' delivery scenarios.

Finally, we also evaluated a 'theoretical' variable beam intensity scenario, for which we assumed no limit on the maximum intensity from e.g., the monitoring system or safety requirements. The maximum beam intensity for this hypothetical scenario ranged from $5.5*10^9$ to $1.2*10^{12}$ protons/s (for 73–229 MeV), and was based on representative transmission data that was obtained by Monte-Carlo beamline simulations [10] and gantry measurements, while considering a realistic 800 nA beam current at the cyclotron [16]. The minimum spot duration was still 3 ms, with spot-wise variable beam intensity. To allow evaluation of clinical plans for this theoretical delivery scenario, no minimum spot weight was imposed.

Results

Plan and dose parameters are listed for all patients in Table 1. The median number of proton spots was reduced from 36108 in the clinical plans to 811, 813, and 2162 in the standard, arc, and arc-shoot-through spot-reduced plans, respectively (i.e., a factor of 17–52), resulting in 18–38 times higher spot weights. Although spots were substantially reduced, dose parameters of spot-reduced plans were typically equal or better than those of the clinical plans. OAR dose parameters in arc-shoot-through plans were sometimes even better compared to the other techniques, but as expected, integral dose was considerably higher. Dose distributions and dose–volume histograms for the treatment plans of patient 1 are depicted in Figure 1.

Figure 2 shows mean DADR values in dose-receiving normal tissue for all treatment plans and delivery scenarios, as FLASH radiotherapy would primarily provide improved normal tissue sparing. The relatively low beam intensity on Gantry 2 resulted in DADRs ranging from 0.7 to 3.0 Gy/s (median over all patient cases). Since beam intensities in this scenario are constant, dose rates depended only on proton energies used, and remained unchanged with increased fraction dose. Considerably higher DADRs were obtained in delivery scenarios with variable beam intensities. For the standard spot-reduced plans delivering a 2-Gy fraction dose, normal tissue dose rates of 4.4, 7.1, and 12.1 Gy/s were observed for the energy-layer-wise, spot-wise, and theoretical spot-wise delivery scenarios, respectively. Comparable DADR values were achieved for arc treatment plans. The arc-shoot-through plans resulted in the highest dose rates, with values of 6.0, 14.1, and 24.4 Gy/s for the abovementioned delivery scenarios. In contrast, comparatively low DADRs (1.7 Gy/s) were obtained for clinical treatment plans, even in the theoretical scenario, as these plans contained many low-weighted spots. Hypofractionation resulted in higher dose rates, especially for the theoretical spot-wise delivery scenario, with arc-shoot-through plans then providing a DADR of 73.2 Gy/s (median over all cases). Variation between patients was limited, whereas considerable spread in DADR values was observed within the normal tissue volume.

Figure 3 shows the corresponding average beam intensity per spot, as a percentage of the maximum available intensity. Since the beam intensity of PSI Gantry 2 is constant, all spots are by definition delivered at maximum intensity. For variable beam intensity scenarios, however, the figure indicates to which extent the achievable intensity is exploited, and how much dose rates can be increased until all spots are delivered at 100% intensity. Average beam intensities, and consequently dose rates, can be increased effectively by using spot-wise beam intensities (instead of energy-layer-wise variation), by spot-reduced treatment planning, and by increasing fraction dose. At the same time, for the hypofractionated scenarios with beam intensities already close to 100%, moving to even higher fraction doses will not have a notable effect on the dose rate.

DADR distributions and histograms for patient 1 are shown in Figure 4, for the hypofractionated theoretical spot-wise delivery scenario. As a reference, DADR distributions for

Table 1. Treatment plan characteristics for a 2 Gy fraction (median values over all patient cases).

Parameter		#	Clinical	Standard spot-reduced	Arc spot-reduced	Arc-shoot-through spot-reduced
Fields			4	4	110	117
Energy layers			206	163	450	117
Spots			36108	811	813	2162
Protons	[$\cdot 10^9$]		92	75	65	114
PTV	$D_{98\%}$ [%]	(4)	93	94	94	93
PTV	Mean [%]	(4)	100	100	100	100
PTV	$D_{2\%}$ [%]	(4)	107	105	105	105
PTV	$V_{95\%}$ [%]	(4)	95	97	97	96
PTV	$V_{107\%}$ [%]	(4)	2	0	1	0
PTV	$CI_{95\%}$	(4)	1.11	1.08	1.07	1.06
CTV	Mean [%]	(4)	100	100	100	100
CTV	$V_{95\%}$ [%]	(4)	99	100	100	100
Eye – left	Mean [%]	(4)	75	70	48	46
Eye – left	$D_{2\%}$ [%]	(4)	95	94	91	91
Eye – right	Mean [%]	(4)	68	64	38	50
Eye – right	$D_{2\%}$ [%]	(4)	90	90	75	82
Lens – left	$D_{2\%}$ [%]	(4)	85	74	54	49
Lens – right	$D_{2\%}$ [%]	(4)	76	69	41	45
Optic nerve – left	$D_{2\%}$ [%]	(4)	103	100	100	101
Optic nerve – right	$D_{2\%}$ [%]	(4)	103	100	100	100
Chiasm	$D_{2\%}$ [%]	(4)	103	100	100	100
Brainstem	$D_{2\%}$ [%]	(4)	64	50	43	47
Spinal cord	$D_{2\%}$ [%]	(3)	0	0	0	0
Cochlea – left	Mean [%]	(4)	15	2	6	15
Cochlea – right	Mean [%]	(3)	4	0	3	4
Lacrimal gland – left	Mean [%]	(3)	65	62	50	43
Lacrimal gland – right	Mean [%]	(3)	51	47	18	46
Parotid gland – left	Mean [%]	(3)	9	2	5	9
Parotid gland – right	Mean [%]	(2)	3	1	1	3
Integral dose	[Gy·mm^3·10^6]	(4)	1.29	1.11	1.07	1.45

Dose parameters are given as a percentage of the prescribed dose.
PTV: planning target volume; CTV: clinical target volume; $CI_{95\%}$: 95% conformity index (i.e., patient $V_{95\%}$ [cm^3]/PTV $V_{95\%}$ [cm^3]). Numbers between brackets indicate number of patients in which the structure was delineated.

simple cases and a clinical delivery are depicted in Figure S3 (Supplementary Material). Dose rate values were distributed inhomogeneously across the patient volume, with highest values generally observed at pencil beam entrance and at the Bragg peak. The histograms indicate that average dose rate values for the PTV and normal tissue were comparable, with more homogenous dose rates in the former.

Discussion

In this study, 3D dose-averaged dose rate distributions have been evaluated for four head-and-neck cases in order to investigate whether such dose rates approach the FLASH domain (>40 Gy/s) when different treatment planning paradigms and delivery scenarios are assumed. To the best of our knowledge, this is the first study of its type.

We found that FLASH dose rates could not be obtained for conventional IMPT treatment plans or current clinical PBS machines. Higher instantaneous dose rates were obtained by increasing the achievable (variable) beam intensity and by using higher proton energies, as beam losses in the beamline and gantry generally decrease with energy [10]. For PBS systems operating with variable beam intensities, dose rates were subsequently increased by using spot-wise intensity variation, spot-reduced treatment planning or hypofractionation. In addition, one could also reduce the minimum required spot duration, but this is similar to increasing the fraction dose, from a dose rate perspective (note that unrestricted spot duration is again equivalent to constant beam intensity). We found that all these strategies were indeed effective, although their impact was limited. For example, we observed that at some point, further hypofractionation, higher beam intensities or spot-wise intensities did not provide any additional improvement in dose rate. In fact, it was only the combination of all strategies (i.e., arc-shoot-through planning together with the hypofractionated theoretical delivery scenario) that resulted in FLASH compatible dose rates. It should be stressed however, that the FLASH dose rates for arc-shoot-through plans came at the cost of substantially higher integral dose, and it remains to be seen whether the actual clinical benefit of FLASH radiotherapy will justify these increased normal tissue doses.

To calculate spatially varying dose rate distributions, we have proposed the 'dose-averaged dose rate' as a metric. As proton spots are delivered in a sequential fashion during PBS proton therapy, with each voxel generally receiving dose from multiple spots, this metric provided a practical method to accumulate dose rates in each voxel while taking into account the 'importance' of each spot. As such it is analogous to calculating dose-averaged linear energy transfer (LET) distributions [17–19]. DADR values were calculated using the mean intensity of a pulsed proton beam (intensity within a pulse is 17.5 times higher) [20], which is in line with beam intensities reported in the initial publications on FLASH radiotherapy [1–4]. However, whether the biological mechanisms responsible for the FLASH effect are adequately captured by this metric is unclear, and this is probably the most important limitation of the current study. Only instantaneous dose rates were considered during DADR calculations, ignoring dead times between spots, which could have

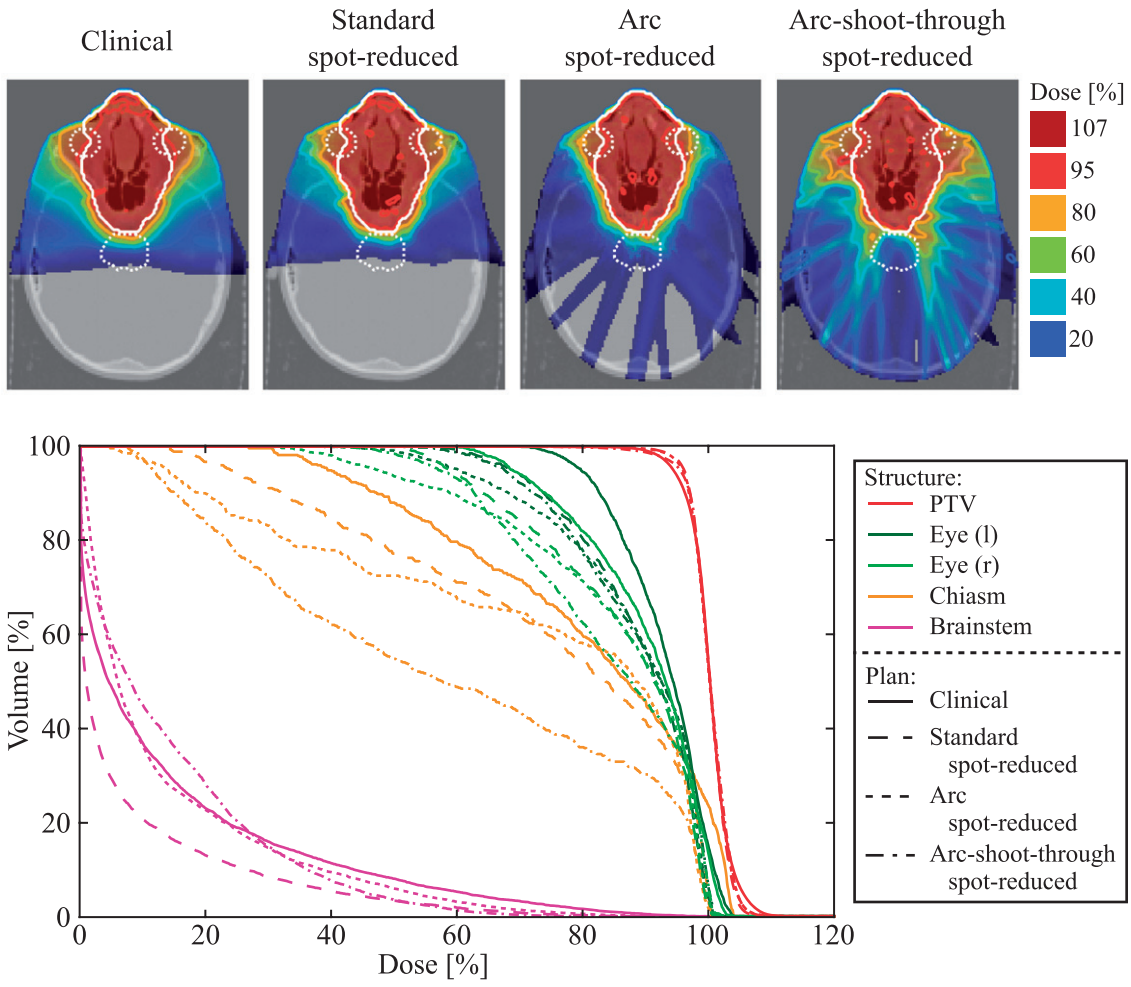

Figure 1. Dose distributions and dose–volume histograms for the different treatment plans of patient 1. White contours indicate the PTV (solid), and eyes and brainstem (dotted).

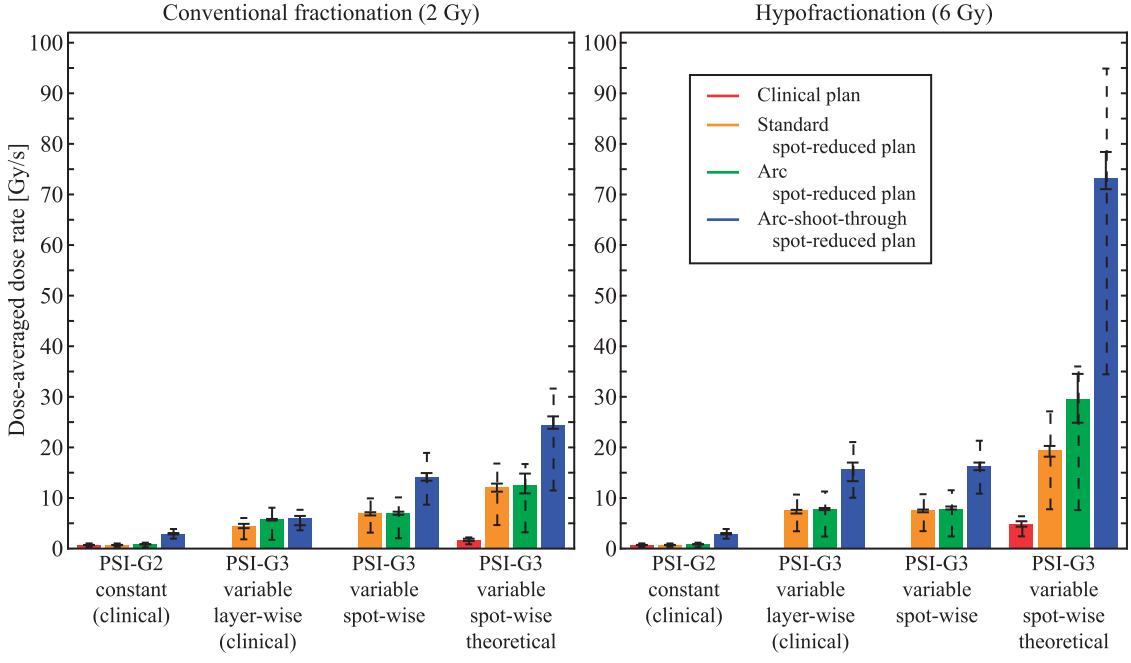

Figure 2. Mean dose-averaged dose rates (DADR) in dose-receiving normal-tissue for the different treatment plans and delivery scenarios (median over all cases). Solid whiskers indicate variation (min/max) in mean DADR between the four cases, dashed whiskers indicate DADR values received by 25% and 75% of the volume (median over all cases). PSI-G2 = PSI Gantry 2; PSI-G3 = PSI Gantry 3.

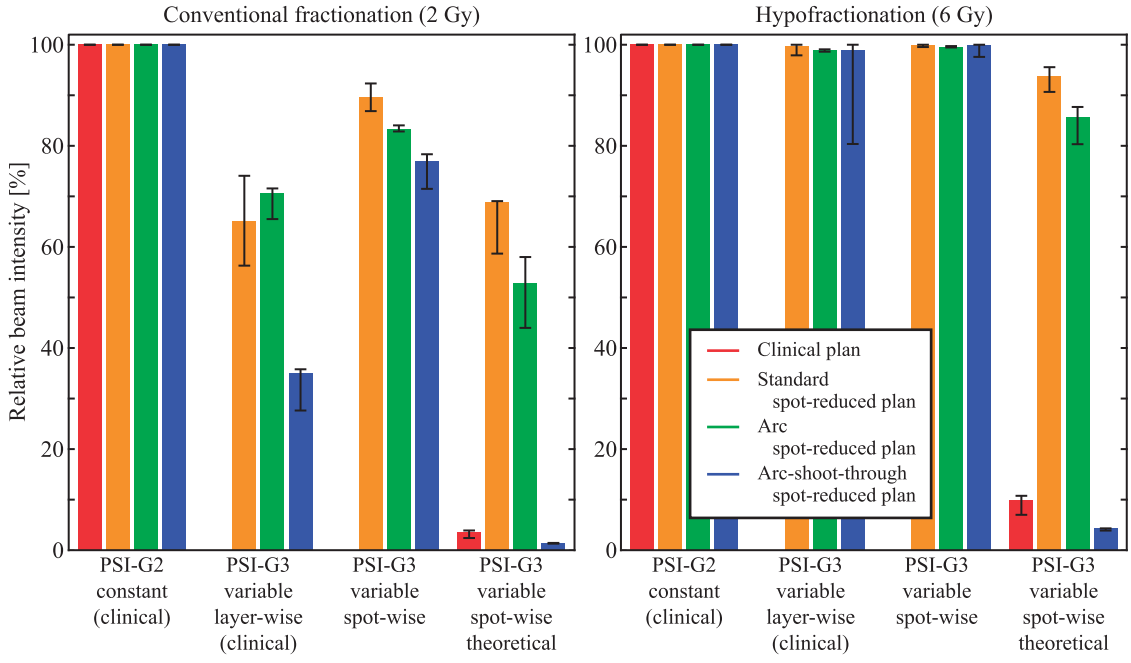

Figure 3. Mean beam intensity per spot, as a percentage of the maximum available beam intensity, for the different treatment plans and delivery scenarios (median over all cases). Whiskers indicate the variation (min/max) between the four cases. PSI-G2 = PSI Gantry 2; PSI-G3 = PSI Gantry 3.

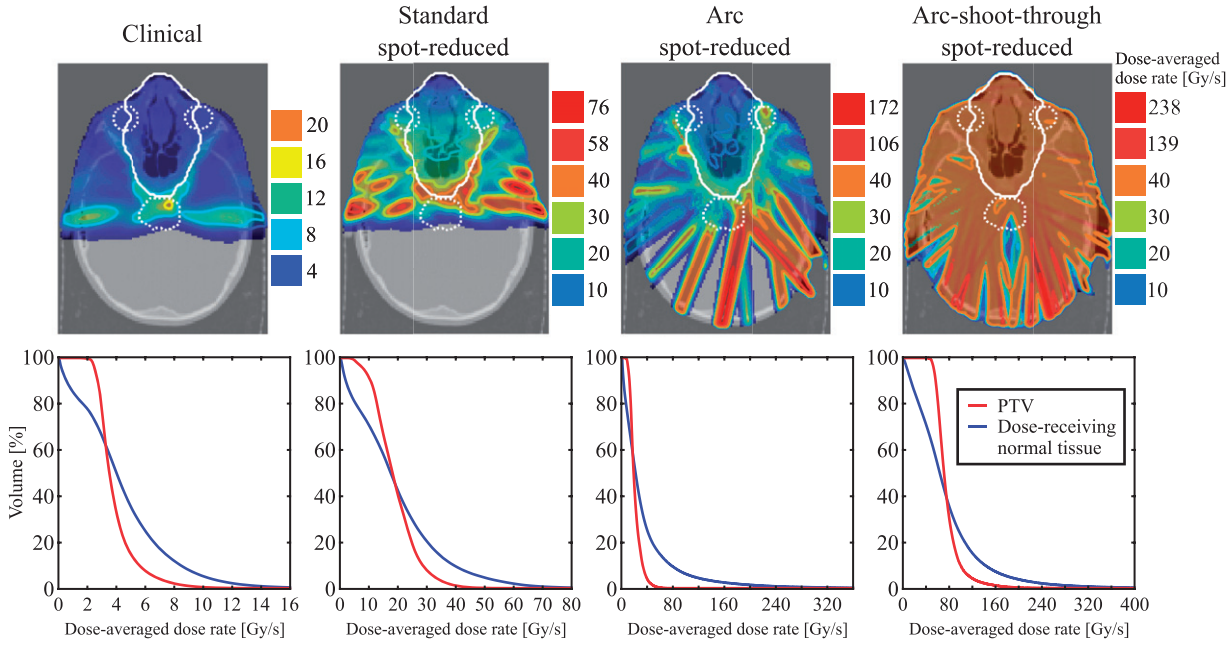

Figure 4. Dose-averaged dose rate (DADR) distributions and histograms for the treatment plans of patient 1, for the theoretical variable beam intensity scenario and 6 Gy fraction dose (hypofractionation). White contours indicate the PTV (solid), and eyes and brainstem (dotted).

resulted in an overestimation of the effective dose rate. With pre-clinical FLASH experiments only using single beams and with a validated radiobiological explanation for the FLASH effect still lacking [1,4,6,7], the impact of dead times between spots on the effective dose rate remains unclear. The current approach was therefore deemed reasonable and appropriate for the purpose of this study. Moreover, simply averaging dose rates over the entire fraction duration as an alternative might not be suitable either, given the complex delivery time-structure as depicted in Figure S4 (Supplementary Material). More radiobiological research is required to better understand time-related aspects of FLASH radiotherapy, and to clarify for example whether there is a threshold dose to trigger the FLASH effect and how long the effect persists. Until then, the dose-averaged dose rates presented in this study should be considered as the best-case scenario.

Spot-reduced treatment plans contained considerably fewer spots than the clinical plans. In this study we confirmed that plan quality was maintained or even improved for these plans (see Table 1 and Figure 1), but we did not examine other aspects such as plan robustness. However, a recent experimental validation showed that such a spot-reduced plan could be delivered with high accuracy on PSI Gantry 2, whilst reducing delivery times per field by

approximately 50%, and that plan robustness was not substantially affected [21]. Nevertheless, for the arc treatment plans, deliverability might be questionable, as we did not consider the actual continuous delivery of these plans with a rotating gantry. A disadvantage of current spot-reduced treatment planning is the relatively long optimization time, requiring 2.1, 3.6, and 2.0 h for optimizing standard, arc, and arc-shoot-through spot-reduced plans. However, spot-reduced planning uses prioritized multi-criteria optimization [22], allowing for fully automated treatment plan generation without user interaction [23]. Incorporating dose rate optimization in the spot-reduced TPS is currently investigated at our institute, as this could for example provide higher dose rates without increasing integral dose, increased dose rate homogeneity, or FLASH dose rates for an increased relative normal tissue volume.

In conclusion, using a new metric (dose-averaged dose rate, or DADR), we question whether instantaneous dose rates exceeding the FLASH threshold (>40 Gy/s) can be achieved with conventional treatment planning techniques and current clinical PBS machines. DADR values could however be increased by using higher and spot-wise variable beam intensities, spot-reduced treatment planning, hypofractionation, and/or higher proton energies in shoot-through mode. Nevertheless, each of these measures was limited in its effectiveness, and only the combination of all provided FLASH compatible instantaneous dose rates for the patient cases studied here.

Disclosure statement

No potential conflict of interest was reported by the authors.

Funding

This work was supported by the EU-H2020 (Horizon 2020 Framework Programme) project 'INSPIRE' (INfraStructure in Proton International REsearch; grant ID: 730983).

References

[1] Favaudon V, Caplier L, Monceau V, et al. Ultrahigh dose-rate FLASH irradiation increases the differential response between normal and tumor tissue in mice. Sci Transl Med. 2014;6:245ra93.

[2] Montay-Gruel P, Petersson K, Jaccard M, et al. Irradiation in a flash: unique sparing of memory in mice after whole brain irradiation with dose rates above 100Gy/s. Radiother Oncol. 2017;124:365–369.

[3] Vozenin M-C, Fornel PD, Petersson K, et al. The advantage of FLASH radiotherapy confirmed in mini-pig and cat-cancer patients. Clin Cancer Res. 2019;25:35–42.

[4] Montay-Gruel P, Bouchet A, Jaccard M, et al. X-rays can trigger the FLASH effect: ultra-high dose-rate synchrotron light source prevents normal brain injury after whole brain irradiation in mice. Radiother Oncol. 2018;129:582–588.

[5] Buonanno M, Grilj V, Brenner DJ. Biological effects in normal cells exposed to FLASH dose rate protons. Radiother Oncol. 2019;139:51–55.

[6] Durante M, Bräuer-Krisch E, Hill M. Faster and safer? FLASH ultra-high dose rate in radiotherapy. Br J Radiol. 2018;91:20170628.

[7] Spitz DR, Buettner GR, Petronek MS, et al. An integrated physico-chemical approach for explaining the differential impact of FLASH versus conventional dose rate irradiation on cancer and normal tissue responses. Radiother Oncol. 2019;139:23–27.

[8] Patriarca A, Fouillade C, Auger M, et al. Experimental set-up for FLASH proton irradiation of small animals using a clinical system. Int J Radiat Oncol Biol Phys. 2018;102:619–626.

[9] Zhang Y, Huth I, Weber DC, et al. A statistical comparison of motion mitigation performances and robustness of various pencil beam scanned proton systems for liver tumour treatments. Radiother Oncol. 2018;128:182–188.

[10] van Goethem MJ, van der Meer R, Reist HW, et al. Geant4 simulations of proton beam transport through a carbon or beryllium degrader and following a beam line. Phys Med Biol. 2009;54:5831–5846.

[11] Lomax A. Intensity modulation methods for proton radiotherapy. Phys Med Biol. 1999;44:185–205.

[12] Lomax AJ, Böhringer T, Bolsi A, et al. Treatment planning and verification of proton therapy using spot scanning: initial experiences. Med Phys. 2004;31:3150–3157.

[13] Wieser H-P, Cisternas E, Wahl N, et al. Development of the open-source dose calculation and optimization toolkit matRad. Med Phys. 2017;44:2556–2568.

[14] van de Water S, Kraan AC, Breedveld S, et al. Improved efficiency of multi-criteria IMPT treatment planning using iterative resampling of randomly placed pencil beams. Phys Med Biol. 2013;58:6969–6983.

[15] Safai S, Bula C, Meer D, et al. Improving the precision and performance of proton pencil beam scanning. Transl Cancer Res. 2012;1:196–206.

[16] Rizzoglio V, Adelmann A, Baumgarten C, et al. Evolution of a beam dynamics model for the transport line in a proton therapy facility. Phys Rev Accel Beams. 2017;20:124702.

[17] Wilkens JJ, Oelfke U. Three-dimensional LET calculations for treatment planning of proton therapy. Z Med Phys. 2004;14:41–46.

[18] Grassberger C, Trofimov A, Lomax A, et al. Variations in linear energy transfer within clinical proton therapy fields and the potential for biological treatment planning. Int J Radiat Oncol Biol Phys. 2011;80:1559–1566.

[19] Unkelbach J, Botas P, Giantsoudi D, et al. Reoptimization of intensity modulated proton therapy plans based on linear energy transfer. Int J Radiat Oncol Biol Phys. 2016;96:1097–1106.

[20] Gomà C, Lorentini S, Meer D, et al. Proton beam monitor chamber calibration. Phys Med Biol. 2014;59:4961–4971.

[21] Belosi MF, de Water SV, Albertini DC, et al. PO-0894: reduced spot number for PBS proton therapy shortens delivery time without dosimetric plan compromise. Radiother Oncol. 2018;127:S474–S475.

[22] Breedveld S, Storchi PRM, Voet PWJ, et al. iCycle: integrated, multicriterial beam angle, and profile optimization for generation of coplanar and noncoplanar IMRT plans. Med Phys. 2012;39:951–963.

[23] Voet PWJ, Dirkx MLP, Breedveld S, et al. Toward fully automated multicriterial plan generation: a prospective clinical study. Int J Radiat Oncol Biol Phys. 2013;85:866–872.